NUMERICAL SIMULATIONS OF AERIAL APPLICATION SYSTEMS: A NEW ENHANCED MODEL

Guillermo A. Hazebrouck[a], **Sergio Preidikman**[a,b,c] **and Julio Massa**[a,b]

[a] *Facultad de Ciencias Exactas Físicas y Naturales, Universidad Nacional de Córdoba, Casilla de Correo 916, 5000 Córdoba, Argentina, jmassa@efn.uncor.edu, http://www.efn.uncor.edu*

[b] *Facultad de Ingeniería, Universidad Nacional de Río Cuarto, Ruta Nacional 36 Km. 601, 5800 Río Cuarto, Argentina, spreidikman@ing.unrc.edu.ar, http://www.ing.unrc.edu.ar*

[c] *CONICET - Consejo Nacional de Investigaciones Científicas y Técnicas, Av. Rivadavia 1917 Buenos Aires, Argentina, http://www.conicet.gov.ar*

Keywords: Aerial application. Drift control.

Abstract. This research provides a computer model that simulates the motion of spherical fluid particles or droplets immersed in a non-uniform unsteady stream caused by the relative motion of a solid body and a fluid. The solution is particularly useful to study and improve the spraying of liquid products through aerial application systems.

The developed method brings together two different models. An aerodynamic model supplies the velocity field to a dynamic model that computes the forces exerted on the fluid particles. The aerodynamic drag and the weight of fluid particles are taken into account by this model. The drag is evaluated by means of an empiric method that considers the local Reynolds number. The numerical simulation of aerial applications systems is emphasized. Some results of this class of application are further presented and discussed.

1 INTRODUCTION

Several kinds of agricultural products, such as herbicides, pesticides and fungicides, have to be sprayed over plantations during different stages of their growth. The composition and application of these liquid solutions has to be carefully controlled in order to spray the product homogeneously over the field. Nowadays, modern spraying-devices provide great control on the mass flux and the size of droplets. However, the use of aerial application systems (see Figure 1) might cause an inhomogeneous dispersion of droplets over the field if they are not properly adapted for a specific purpose. Among the main variables to deal with are the size and initial velocity of droplets, the airspeed and altitude of the aircraft, the external shape of the aircraft, the position of the spraying-devices, the composition of the product of application and the atmospheric conditions.

The aim of this research is to provide an enhanced version of the computer model presented on reference Hazebrouck et al. (2010b). This new model will be capable of managing all variables before mentioned in order to predict both, the motion of droplets in the air and the position at which they reach the ground. The introduction of a model of droplets will be considered at first, followed by the development of a method to calculate the exerted forces. Later on, the equation of motion of droplets will be developed and coupled to an aerodynamic model. Finally, several examples picturing results will be presented and some possible solutions to typical problems will be discussed.

Although in this research the aerial application of droplets will be emphasized, the developed method can be easily generalized to study the motion of any kind of spherical particles located inside an unsteady and nonuniform fluid stream caused by the motion of a solid body.

Figure 1: Mist of droplets emitted from an airplane.

1.1 Characteristic of the droplets

Droplets emitted from aerial application systems are formed after a complex physical process that depends on a variety of variables. As it can be seen in Figure 2a, “primary droplets” released from sprayers into the airstream deform due to the aerodynamic pressure around them. Depending on how high the aerodynamic pressure and the surface tension are, this deformation might cause droplets to become membranes. When this phenomenon occurs, the splitting of droplets is imminent, and as result many smaller “secondary droplets” will come to replace primary droplets. This process is known as “shattering of droplets”.

For the aerial application purpose the most important characteristic of droplets is their size. Controlling this parameter is not an easy task because it depends on a large quantity of variables;

nevertheless it has been the subject of many researches, as for example those done by Clayton and by Hewitt (1998). Since tiny droplets are much more stable than big ones, only an important increase on the airspeed might cause secondary droplets to shatter for a second time, and therefore their size and shape remain virtually invariable after they are formed.

Briefly, the main variables that affect the size of secondary droplets are the airspeed, the size of primary droplets and the composition of the product. For standard application purpose the size of secondary droplets is normally set between 200µm and 600µm diameter. Although not all droplets will be of the same size, it is always desired to obtain a narrow spectrum, as it can be seen in Figure 2b.

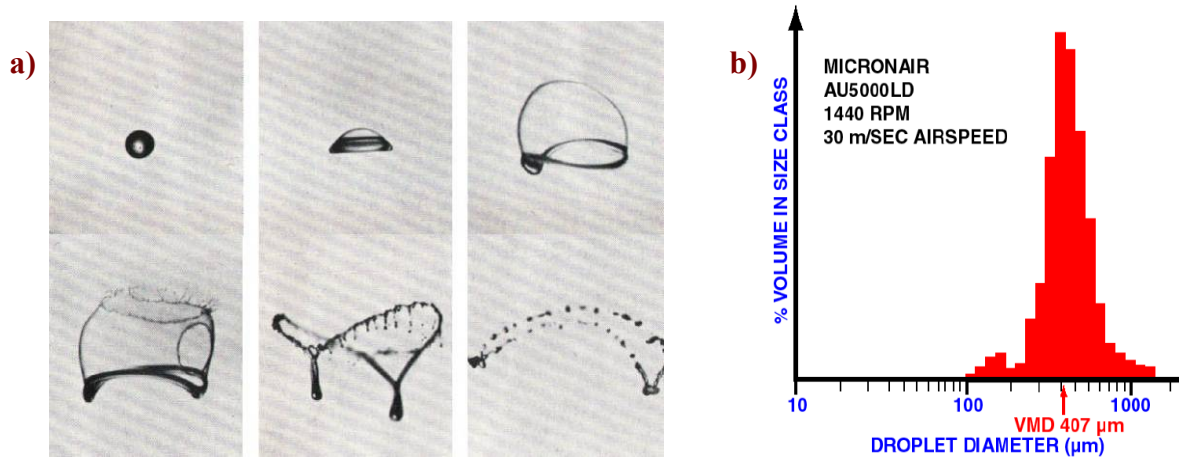

Figure 2: a) "Primary droplets" released into the airflow split into smaller "secondary droplets". b) Spectrum of spray droplets.

1.2 Mechanical model of the droplets

Based on the hypothesis that secondary droplets are rapidly established and stable, they will be modeled as uniform rigid spheres for any aerodynamic requirements. No physical or thermodynamic process involving the change of size, shape or composition of droplets during their fall will be considered. In addition to that, rotational motion will be completely ignored. Thus, droplets will be modeled as point particles with finite mass no moments of inertia.

2 DYNAMICS OF THE DROPLETS

Two forces are exerted on droplets during their fall through the air. The first one is due the gravity field and the second one is purely aerodynamic. The gravity force (weight) can be completely evaluated through the mass of the particle. The drag force, on the other hand, requires the introduction of an aerodynamic model to be evaluated.

In this research particles will be considered as moving inside a locally uniform airstream, and therefore the local velocity of the air will suffice to determine the direction of the drag force. Additionally, since the motion of particles relative to the air will not modify the velocity field, no aerodynamic interaction between particles will be taken into account. Although these restrictions might seem severe, they provide a simplified version of a problem that would be tremendously complex to solve under more realistic circumstances.

2.1 Drag force exerted on a spherical body inside a uniform airstream

Evaluating the drag force exerted on spherical bodies moving inside a uniform airstream has been subject of innumerable investigations and experiments in the past, and for that reason a great amount of empiric information is available about the topic.

As with any other aerodynamic force, the drag force is traditionally written in terms of the free stream dynamic pressure q, the characteristic surface S, and an aerodynamic coefficient C_D:

$$\|\mathbf{D}\| = q\,S\,C_D \tag{1}$$

The free stream dynamic pressure is a function of the free stream density ρ and the free stream velocity ${}^{\mathcal{P}}\mathbf{V}^C$:

$$q = \frac{1}{2}\rho\left\|{}^{\mathcal{P}}\mathbf{V}^C\right\|^2 \tag{2}$$

The vertical bars represent the Euclidean norm, the right superscript C makes reference to the airstream and the left superscript $\mathcal{P}$ indicates that the velocity is being evaluated with respect to a reference frame attached to the particle.

As it can be seen in Figure 3, the direction of the drag force is always coincident with that of the free stream velocity, and therefore we can write:

$$\mathbf{D} = \frac{1}{2}\rho S C_D\left\|{}^{\mathcal{P}}\mathbf{V}^C\right\|{}^{\mathcal{P}}\mathbf{V}^C \tag{3}$$

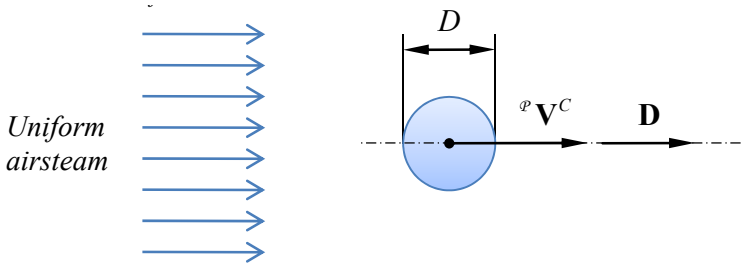

Figure 3: Drag acting on a particle immersed in a uniform airstream.

The drag coefficient is a function of the free stream Reynolds number Re:

$$Re = \frac{D\rho}{\mu}\left\|{}^{\mathcal{P}}\mathbf{V}^C\right\| \tag{4}$$

where D is the diameter of the sphere and μ the free stream viscosity. This relationship has been plotted by Zahm (see Zahm, 1926) according to experimental results, as it can be seen in Figure 4.

There is not a unique mathematical expression of the function $C_D(Re)$ covering the whole domain and that is due to the existence of several complex aerodynamic phenomena such as boundary layer separation and compressibility effects. For a low Reynolds number (less than 0.2) the Stokes theory provides a great approximation to the drag coefficient:

$$C_D = \frac{24}{Re} \tag{5}$$

For Reynolds numbers greater than 0.2 and up to 200,000, the interpolating function devised by Zahm (see Zahm, 1926) lies fairly close to the experimental data:

$$C_D = \frac{28}{Re^{0.85}} + 0.48 \tag{6}$$

Droplets emitted from standard aerial application systems will hardly reach a maximum Reynolds number of 3500, and therefore equations (5) and (6) suffices. In fact, for a speed of 150 kts, sea level conditions and a particle of 600μm diameter, one finds a Reynolds number of:

$$Re = 3163 \tag{7}$$

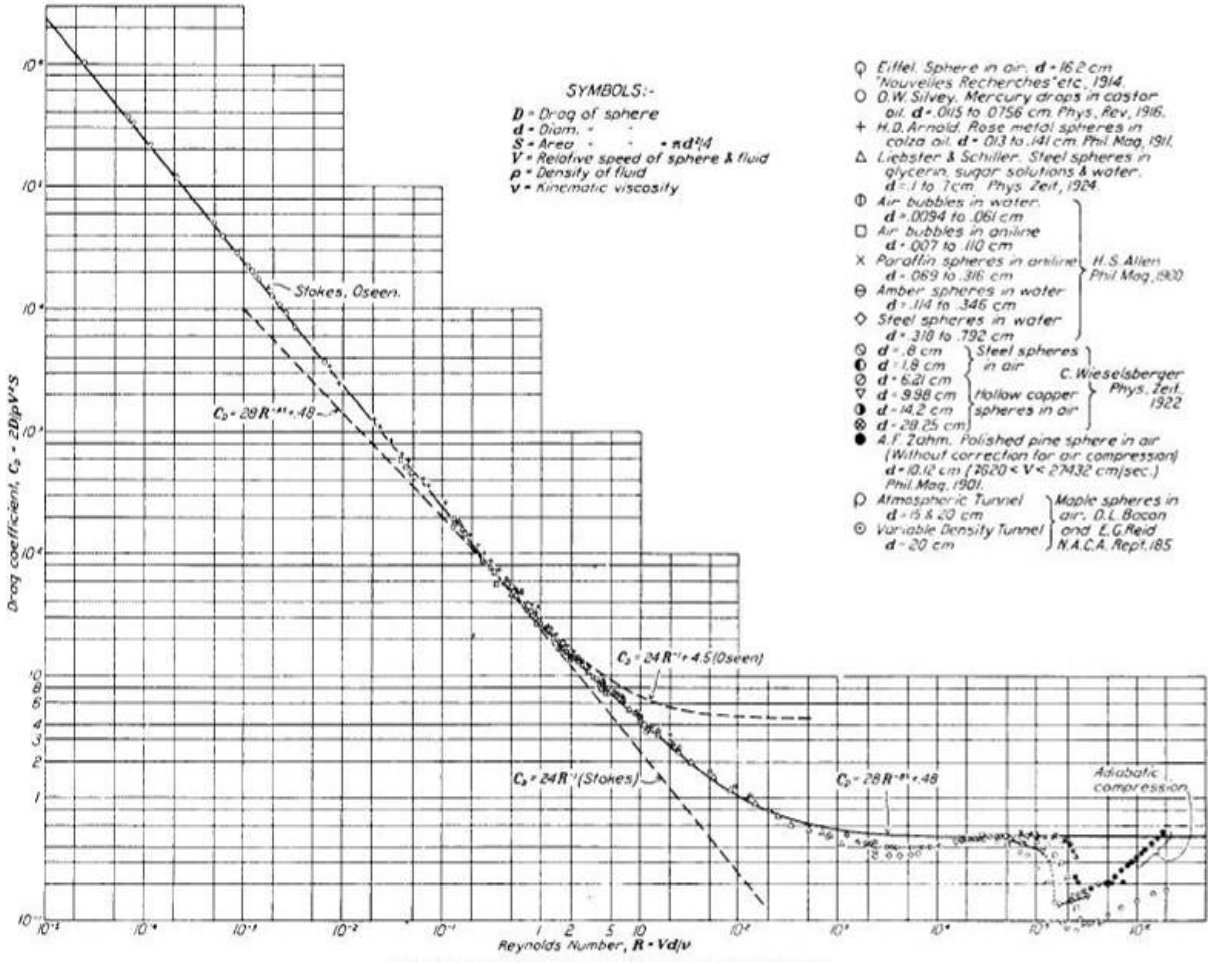

Figure 4: Drag coefficient for a sphere versus Reynolds number (see Zahm, 1926).

2.2 Kinematics of fluid particles moving inside a non-uniform airstream

Figure 5 depicts the free-body diagram of a spherical particle moving inside an airstream with three degrees of freedom and subject to aerodynamic and gravitational forces. Note that two different reference frames, $\mathcal{P}$ and $\mathcal{R}$, as well as a set of orthogonal unit vectors have been introduced to develop the kinematics of the model. Reference frame $\mathcal{P}$ is attached to the particle, while reference frame $\mathcal{R}$ is considered as an inertial reference. Point P is fixed to the center of the sphere, and point O is fixed to $\mathcal{R}$. Unit vector $\hat{\mathbf{c}}$ is vertical.

The airstream velocity with respect to the particle, ${}^{\mathcal{P}}\mathbf{V}^{C}$, can be written in terms of the airstream velocity with respect to the inertial reference frame, ${}^{\mathcal{R}}\mathbf{V}^{C}$, and the "absolute" velocity of the particle, ${}^{\mathcal{R}}\mathbf{V}^{P/O}$:

$$ {}^{\mathcal{P}}\mathbf{V}^{C} = {}^{\mathcal{R}}\mathbf{V}^{C} - {}^{\mathcal{R}}\mathbf{V}^{P/O} \tag{8} $$

The velocity an acceleration of the particle with respect to the inertial reference frame will be equal to the first and second time derivatives of the position vector $\mathbf{P}^{P/O}$, respectively; i.e.:

$$ {}^{\mathcal{R}}\mathbf{V}^{P/O} = {}^{\mathcal{R}}\dot{\mathbf{P}}^{P/O} \tag{9} $$

$$ {}^{\mathcal{R}}\mathbf{a}^{P/O} = {}^{\mathcal{R}}\ddot{\mathbf{P}}^{P/O} \tag{10} $$

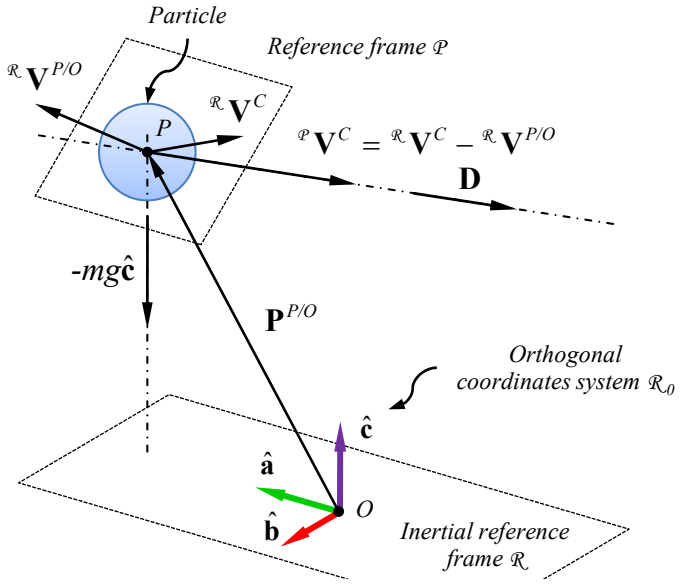

Figure 5: Free-body diagram of a particle moving inside an airstream.

2.3 Dynamics of spherical particles moving inside a non-uniform airstream

According to Equations 3 and 8, the drag force exerted on the particle will be equal to:

$$\mathbf{D} = \frac{1}{2}\rho S C_D \left\| {}^{\mathcal{R}}\mathbf{V}^{C} - {}^{\mathcal{R}}\mathbf{V}^{P/O} \right\| \left({}^{\mathcal{R}}\mathbf{V}^{C} - {}^{\mathcal{R}}\mathbf{V}^{P/O} \right) \tag{11}$$

It might be noted that, according to our model, all free stream parameters are evaluated in the position in which the particle is located. This indicates that the airstream is being considered as locally uniform, even though it is macroscopically nonuniform. This assumption can be accepted because each particle occupies only a tiny region inside the airstream, wherein the velocity gradient does not cause an important change of velocity.

Since the velocity field ${}^{\mathcal{R}}\mathbf{V}^{C}$ varies in space and time and the drag coefficient depends on the relative velocity ${}^{\mathcal{P}}\mathbf{V}^{C}$ trough the Reynolds number, the drag force is in general a function of the position of the particle, the absolute velocity of the particle and the time t, i.e.:

$$\mathbf{D} = \mathbf{D}\left(\mathbf{P}^{P/O}, {}^{\mathcal{R}}\mathbf{V}^{P/O}, t \right) \tag{12}$$

The total external force applied on the particle will be equal to:

$$\mathbf{F} = m\mathbf{g} + \mathbf{D} \tag{13}$$

where $\mathbf{g}$ represents the gravitational acceleration, which is equal to $-g\hat{\mathbf{c}}$, and m the mass of the particle.

According to the law of motion and Equation 13, the acceleration of the particle subject to force $\mathbf{F}$ with respect to the inertial reference frame will be equal to:

$${}^{\mathcal{R}}\mathbf{a}^{P/O} = \mathbf{g} + \frac{1}{m}\mathbf{D} \tag{14}$$

2.4 Velocity field of the airstream ${}^{\mathcal{R}}\mathbf{V}^{C}$

Up to now, the dynamics of particles has been analyzed without concern of the velocity field. Evaluating the velocity field is not a minor problem. In fact, this is the when an aerodynamic model has to be developed and coupled to the current model of particles.

Since the development of an aerodynamic model to study aerial application systems has already been subject of a previous publication, we ask the reader to direct the attention to Chapter 2 of reference Hazebrouck et al. (2010b).

Based on the referred model, the velocity field at position $\mathbf{P}^{P/O}$ and time t will be obtained after summing the velocities associated to each vortex ring:

$$
{}^{\mathcal{R}}\mathbf{V}^{C}\left(\mathbf{P}^{P/O},t\right)=\sum_{j=1}^{N_{BR}}G_j\sum_{k=1}^{4}\frac{1}{4\pi}\frac{\mathbf{L}_{jk}\times\mathbf{r}_{1jk}}{\left\|\mathbf{L}_{jk}\times\mathbf{r}_{1jk}\right\|^2}\left[\mathbf{L}_{jk}\bullet\left(\hat{\mathbf{e}}_{1jk}-\hat{\mathbf{e}}_{2jk}\right)\right]+
\sum_{p=1}^{N_{FR}}G_p\sum_{k=1}^{4}\frac{1}{4\pi}\frac{\mathbf{L}_{pk}\times\mathbf{r}_{1pk}}{\left\|\mathbf{L}_{pk}\times\mathbf{r}_{1pk}\right\|^2}\left[\mathbf{L}_{pk}\bullet\left(\hat{\mathbf{e}}_{1pk}-\hat{\mathbf{e}}_{2pk}\right)\right]+{}^{\mathcal{R}}\mathbf{V}^{C\infty}
\tag{15}
$$

where vector ${}^{\mathcal{R}}\mathbf{V}^{C\infty}$ represents the free stream velocity, N_{FR} the number of free rings and N_{BR} the number of bounded rings. All other vectors and subscripts of Equation 15 are represented in Figure 6.

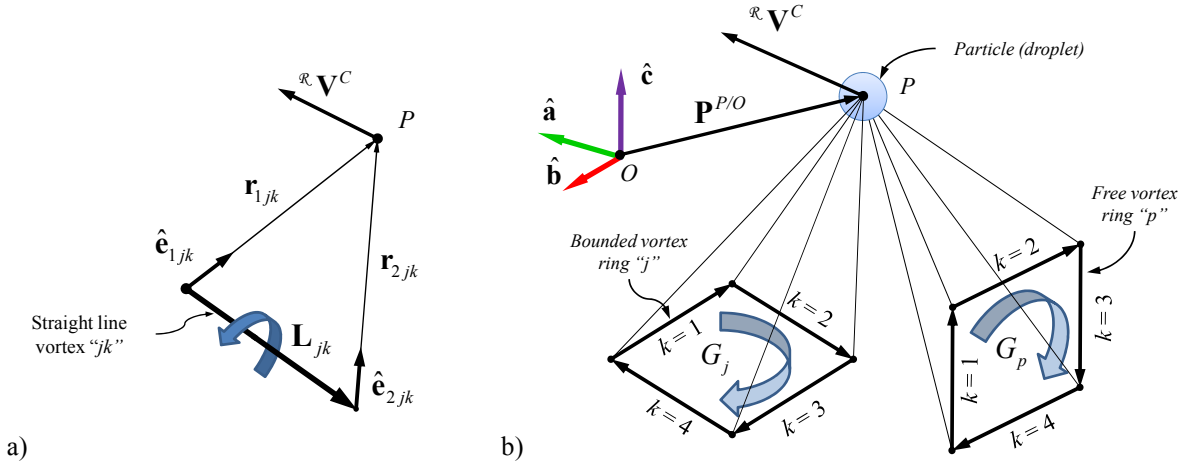

Figure 6: Vectors and subscripts used in Equation 15. a) Finite straight line vortex. b) Vortex rings.

3 NUMERICAL INTEGRATION OF THE EQUATION OF MOTION

Equations 10 and 14 form together a set of three scalar second order ordinary differential equations that describe the motion of each particle inside the airstream:

$$
{}^{\mathcal{R}}\ddot{\mathbf{P}}^{P/O}=\mathbf{g}+\frac{1}{m}\mathbf{D}
\tag{16}
$$

Because of the aerodynamic model that has been implemented, these equations have to be numerically integrated. References Carnahan et al. (1969) and Preidikman (1998) provide the numerical method used in this research.

Independently of which numerical method has been chosen, there are two different schemes to solve Equations 16. If particles are emitted in the unsteady state, they should be integrated in simultaneous with the wake convection. If, on the other hand, particles are emitted in the steady state, they can be separately integrated after the wake is totally convected. Both schemes can be implemented in a very similar way; however, the effort required by the CPU differs in each case.

Provided that the number of numerical operations required to integrate Equations 16 is proportional to the number of vortex rings, the time required to complete each time-step increases while the wake is being convected. Due to the fact that particles emitted from aerial

application systems will hardly reach the ground before the aircraft is at least 60 meters away, a long wake is normally required to evaluate the velocity. This is the reason why this kind of simulations might take several hours to complete when running in a standard CPU.

3.1 The initial conditions

Several spraying-devices can be simulated just by changing the initial velocity of particles. Figure 7 depicts two examples that clearly show this idea. In the first one, starting points are located around circles and particles are only emitted in radial directions. This case represents very well the effect of wind turbines with profiled air deflectors. In the second example, a group of particles are emitted from a same starting point and the initial velocity has both, radial an axial components. This case very well represents the effect of conical nozzles.

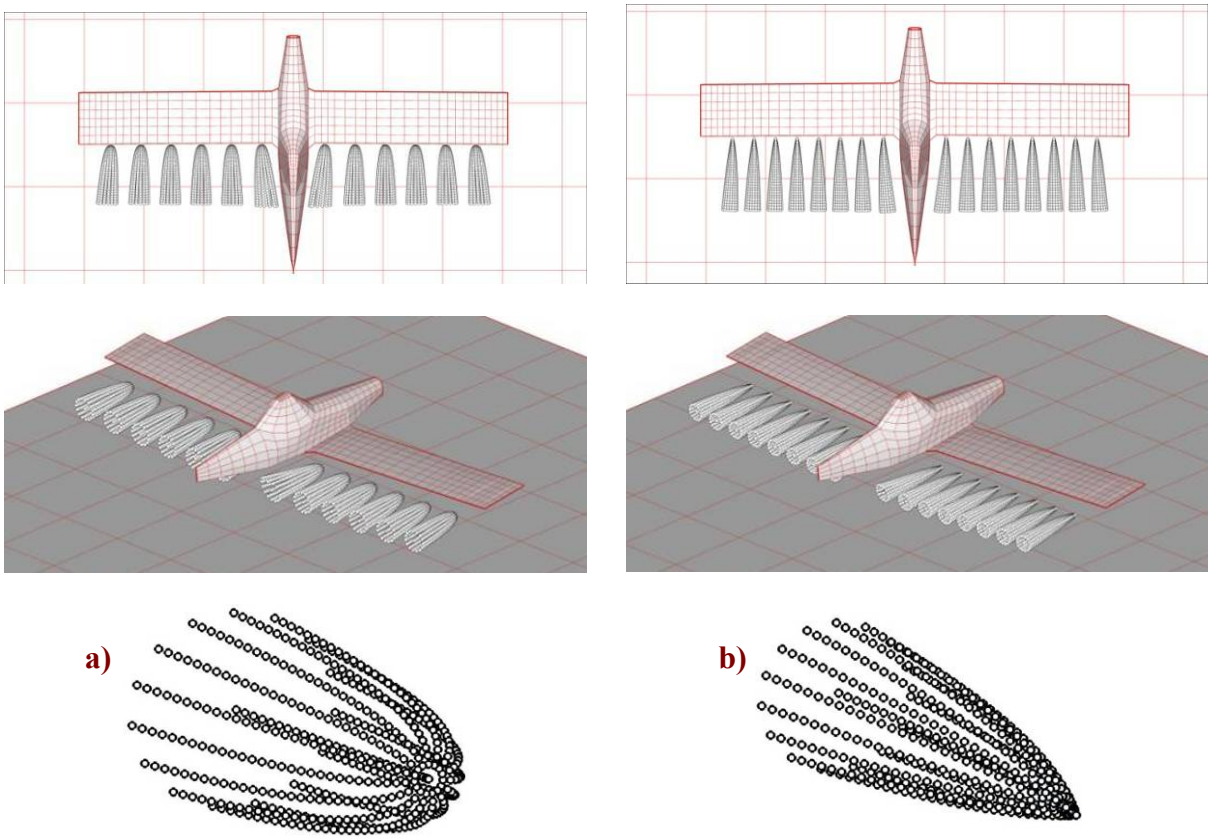

Figure 7: Several spraying-devices can be simulated by changing the initial velocity given to the particles. a) Simulation of wind turbines. b) Simulation of conical nozzles.

4 RESULTS

In this section five different examples will be presented. Figures 7 to 10 show the results for the first two of them. In both cases the aircraft is flying at the same condition and droplets come out from the spraying-devices at the same initial speed and position (note that all common data is outlined on Table 1). The only difference between the two cases is the size of droplets (particular data is outlined on Table 2). Comparing Figures 8 and 11 it can be seen that small droplets remain longer in the air than big ones, and that they are easily dragged by the wingtip vortices.

Result of Example 1 presented in Figure 8 pictures the typical problem associated to aerial application systems. If the external spraying-devices are located too close to the wingtips,

droplets coming out from them will spin around the wingtip vortices before reaching the ground. This phenomenon causes droplets to stay longer in the air. It can be seen that the upwards velocity of the airstream in these regions makes some particles gain altitude instead of falling to the ground. The longer the droplets hover in the air, the less chances they reach the ground in the desired region with the desired composition.

A possible solution to this problem has been considered in the third example. Note from Figure 13 that all spraying-devices have been moved closer to the fuselage, and that another pair of sprayers has been added.

Flight conditions	
Aircraft	AT-502 (wing only) Aspect ratio Æ = 8.486
Wingspan	15.52m (42 panels)
MAC	1.829m (6 panels)
Altitude	3m
True airspeed	58.33m/s ≈ 113kts
Wight	Critical condition : 95% of MPL + full fuelled
Wake convection & Simulation parameters	
Wake life-period	250 time-steps → 1.31s → 76m
Total simulation time	270 time-steps → 1.41s
Time-step	0.005225s
Cut-off	1×10^{-5}
Ground	
Dimensions	100m x 25m (flat surface)
Panels	35 x 12
Atmospheric conditions	
Density	1.225 kg/m³ (sea level)
Viscosity	1.789×10^{-5} kg/ms (sea level)

Table 1: Common data used to simulate examples 1, 2 and 3.

Droplets & Spraying	Example 1	Example 2	Example 3
Droplets diameter	200µm (homogeneous)	500µm (homogeneous)	200µm (homogeneous)
Product density	1000kg/m³	1000kg/m³	1000kg/m³
Initial speed	27m/s (radial only)	27m/s (radial only)	25m/s (radial only)
Nº of spraying-devices	12	12	14
Nº of droplets/device	16	16	16
Time-step	0.001750s	0.001750s	0.001750s
Simulation time	765 time-steps	765 time-steps	765 time-steps

Table 2: Particular data used to simulate examples 1, 2 and 3.

4.1 Example 1: Spraying of 200µm diameter droplets

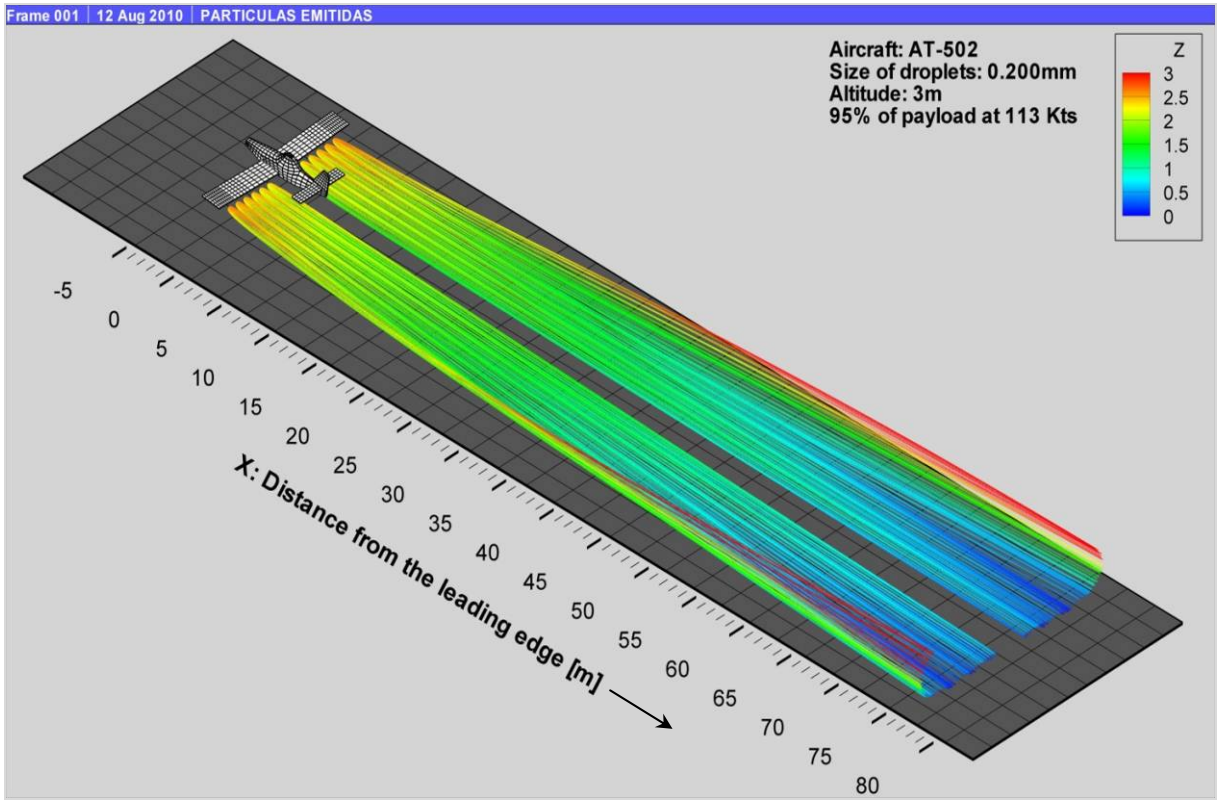

Figure 8: Simulation of 200µm diameter droplets emitted from an aircraft equipped with wind turbines (steady state).

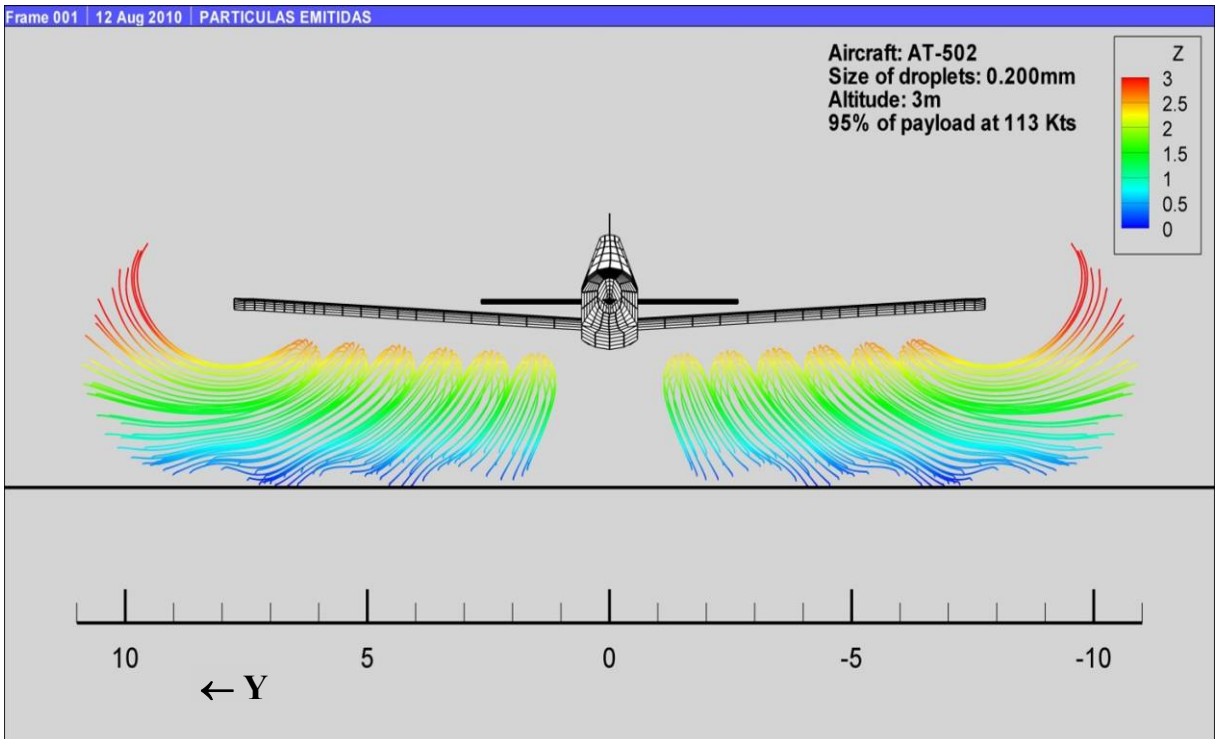

Figure 9: Droplets are dragged by the wingtip vortices (front view of Figure 7).

4.2 Example 2: Spraying of 500µm diameter droplets

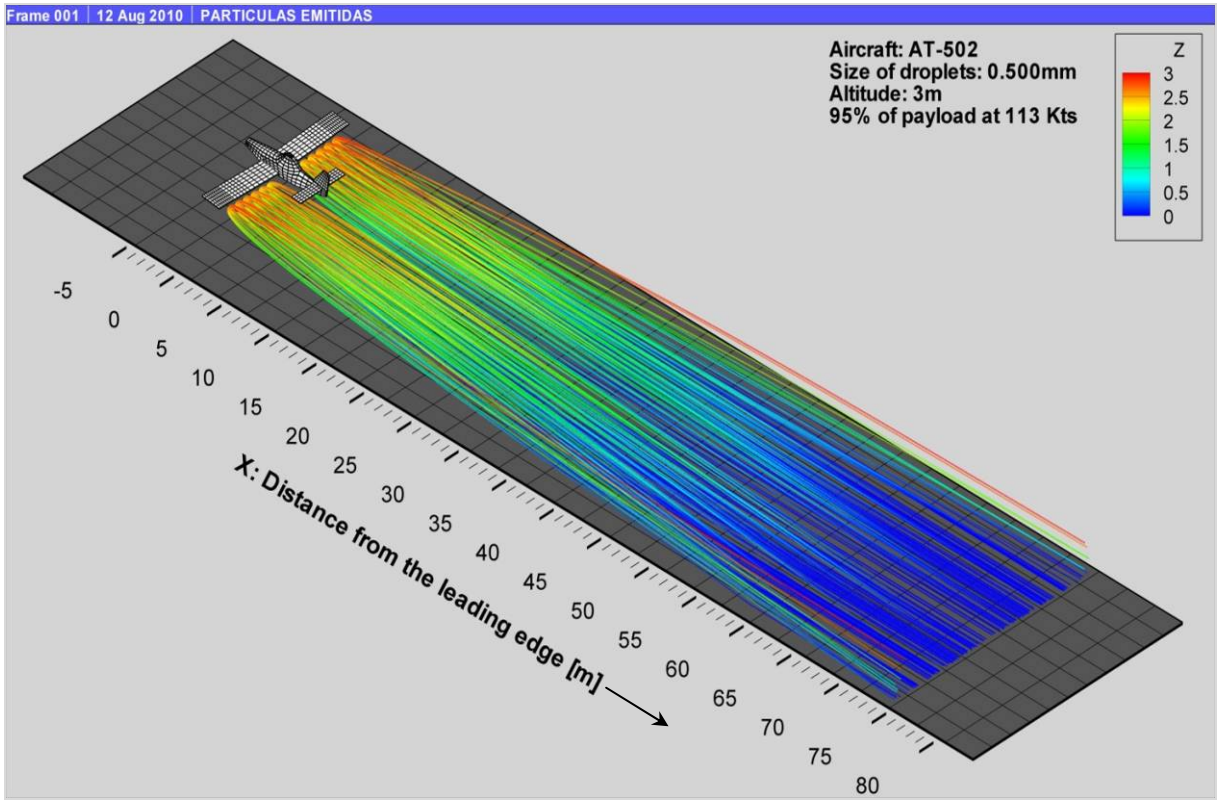

Figure 10: Simulation of 500µm diameter droplet emitted from an aircraft equipped with conical nozzles (steady state). Blue particles are already landed.

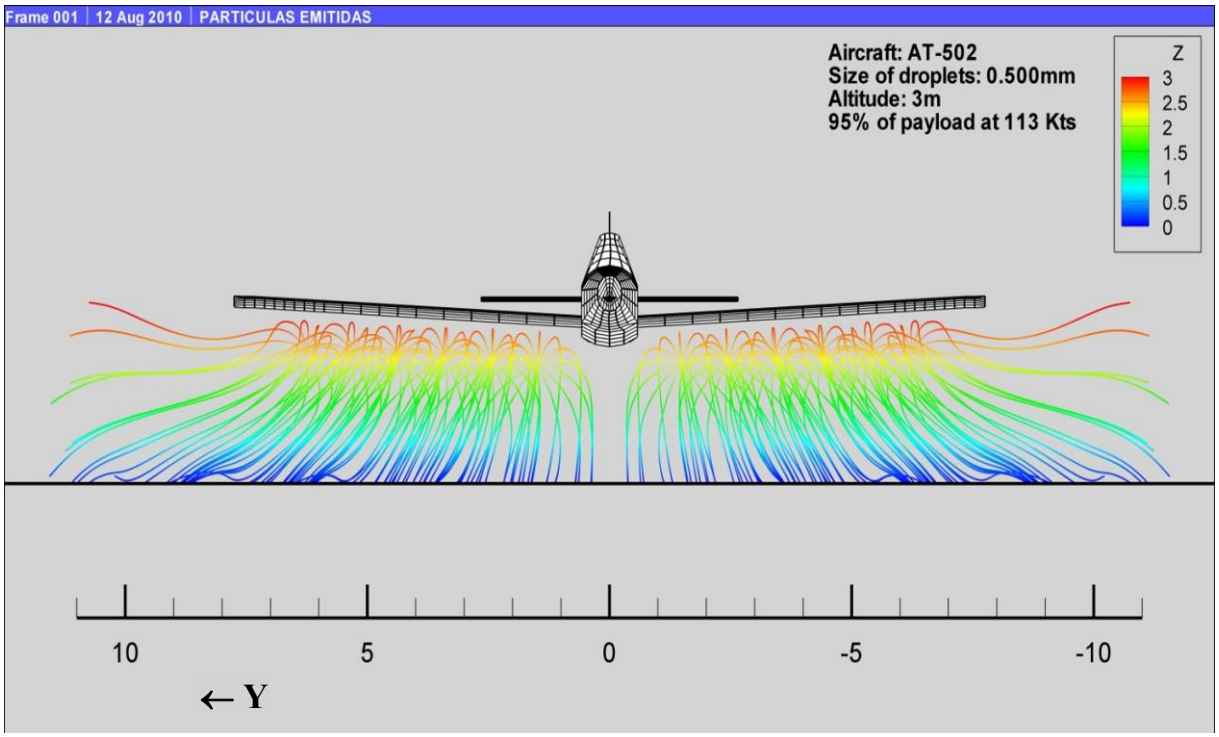

Figure 11: Droplets are dragged by the wingtip vortices (front view of Figure 10).

4.3 Example 3: Spraying of 200µm diameter droplets (enhanced solution)

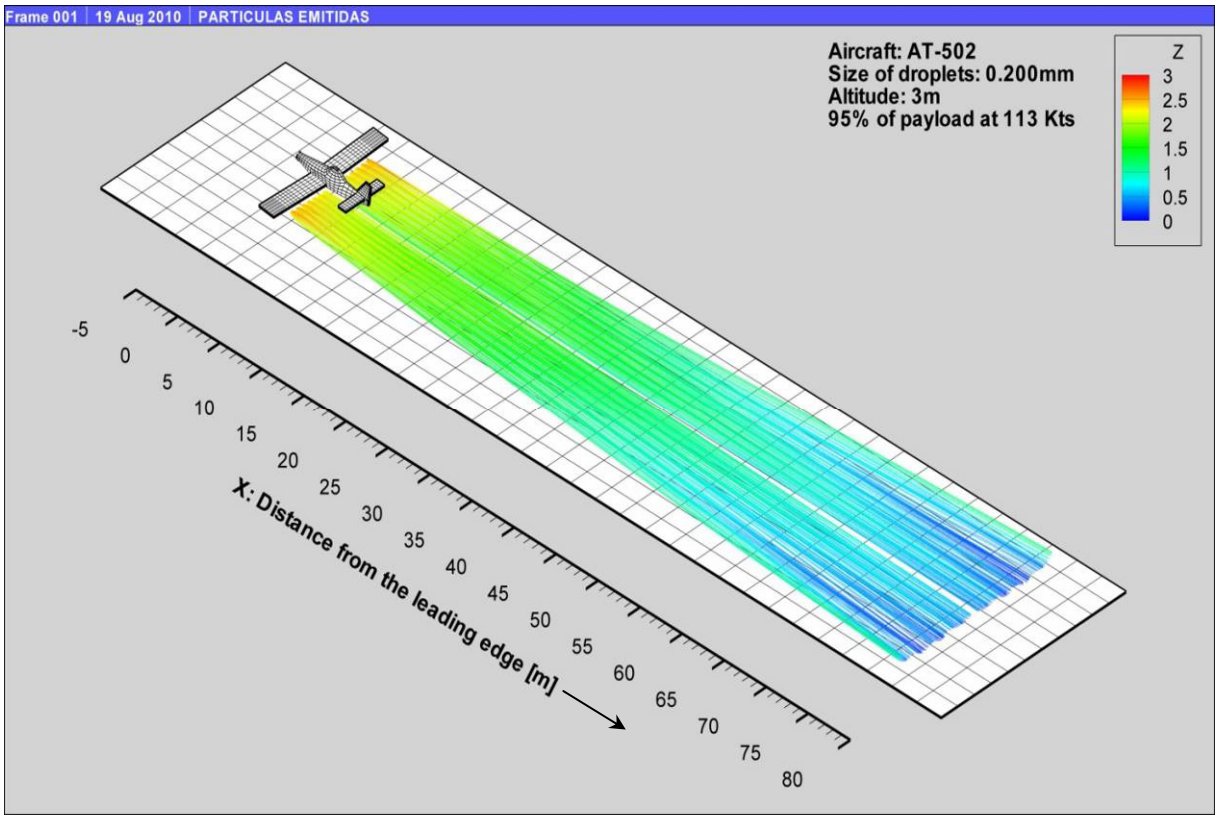

Figure 12: Possible solution to problem detected in Example 1.

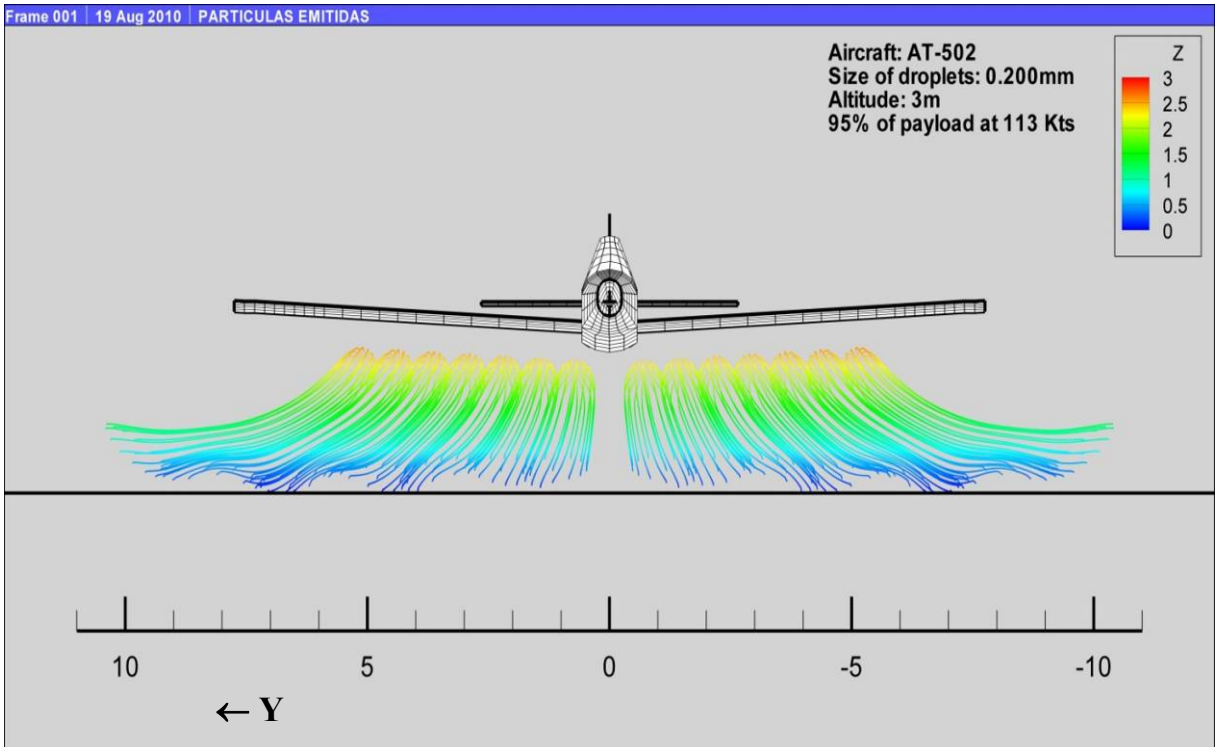

Figure 13: Possible solution to problem detected in Example 1.

4.4 Example 4: Influence of the fuselage on the motion of droplets

As it can be seen in Figure 14, the addition of the fuselage causes particles to leave the aircraft in a considerably different way. Because of the gradual narrowing of the tail, the airstream changes its direction in that region and thus particles are forced to move closer to the plane of symmetry. Since droplets are now covering the central region, there is no need to locate an extra spraying-device under the fuselage. Moreover, if the spraying-devices are located to close to the plane of symmetry, droplets may even cross over it, as depicted in Figure 14.

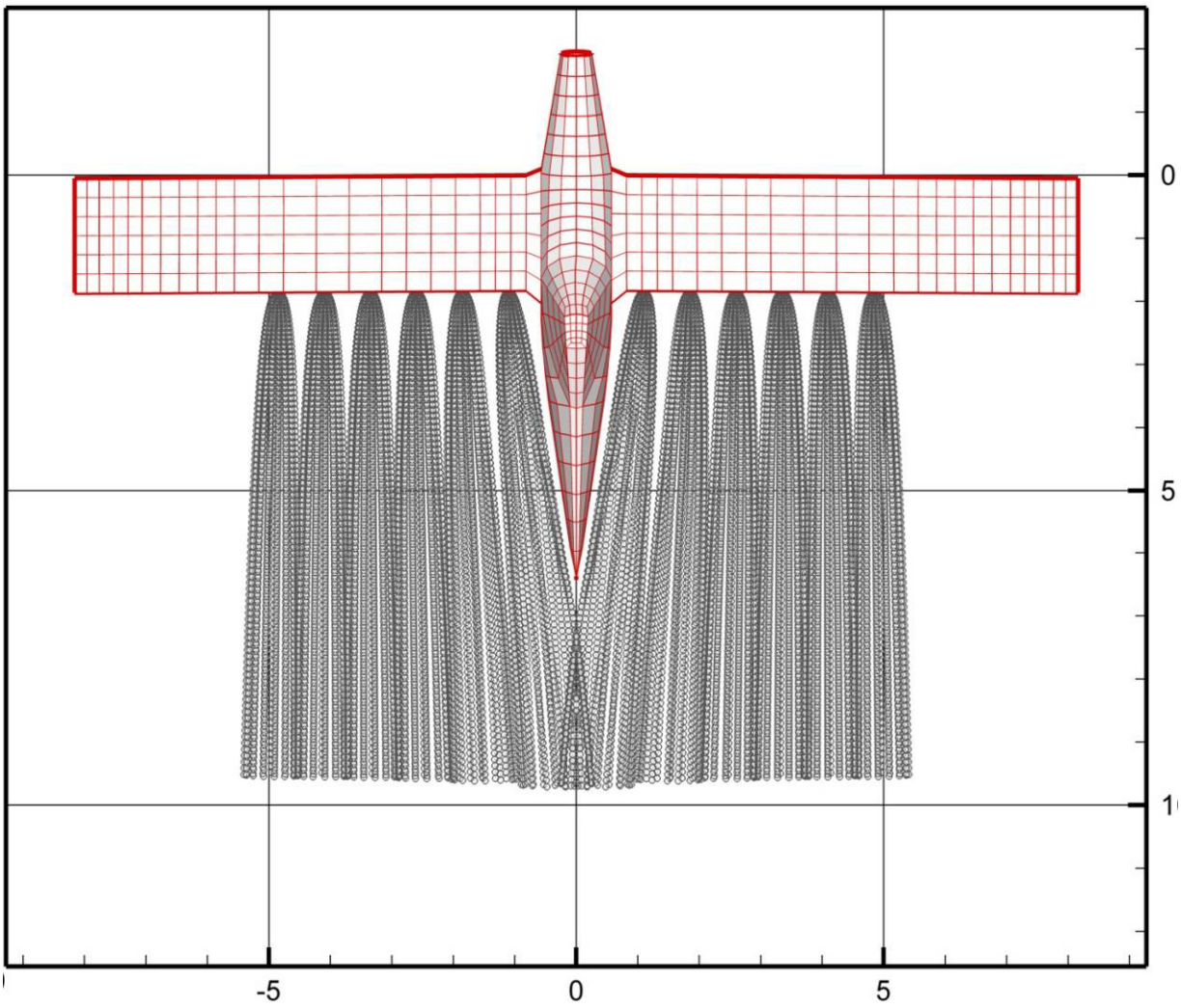

Figure 14: Effect of fuselage on the motion of droplets.

4.5 Brief discussion about the consequences of using different wing-fuselage configurations

The position of the wing with respect to the fuselage plays an important role in determining the efficiency of aerial application systems. Although it is known that low-wing airplanes behave more efficiently than high-wing airplanes when flying at low altitude (see Hazebrouck et al. 2010b), high-wing airplanes might be capable of providing a more homogeneous dispersion of droplets on the ground. In fact, as this kind of configuration allows the spraying-devices to be located further from the wing, droplets are not strongly dragged by the wingtip vortices. This can be seen in Figure 15.

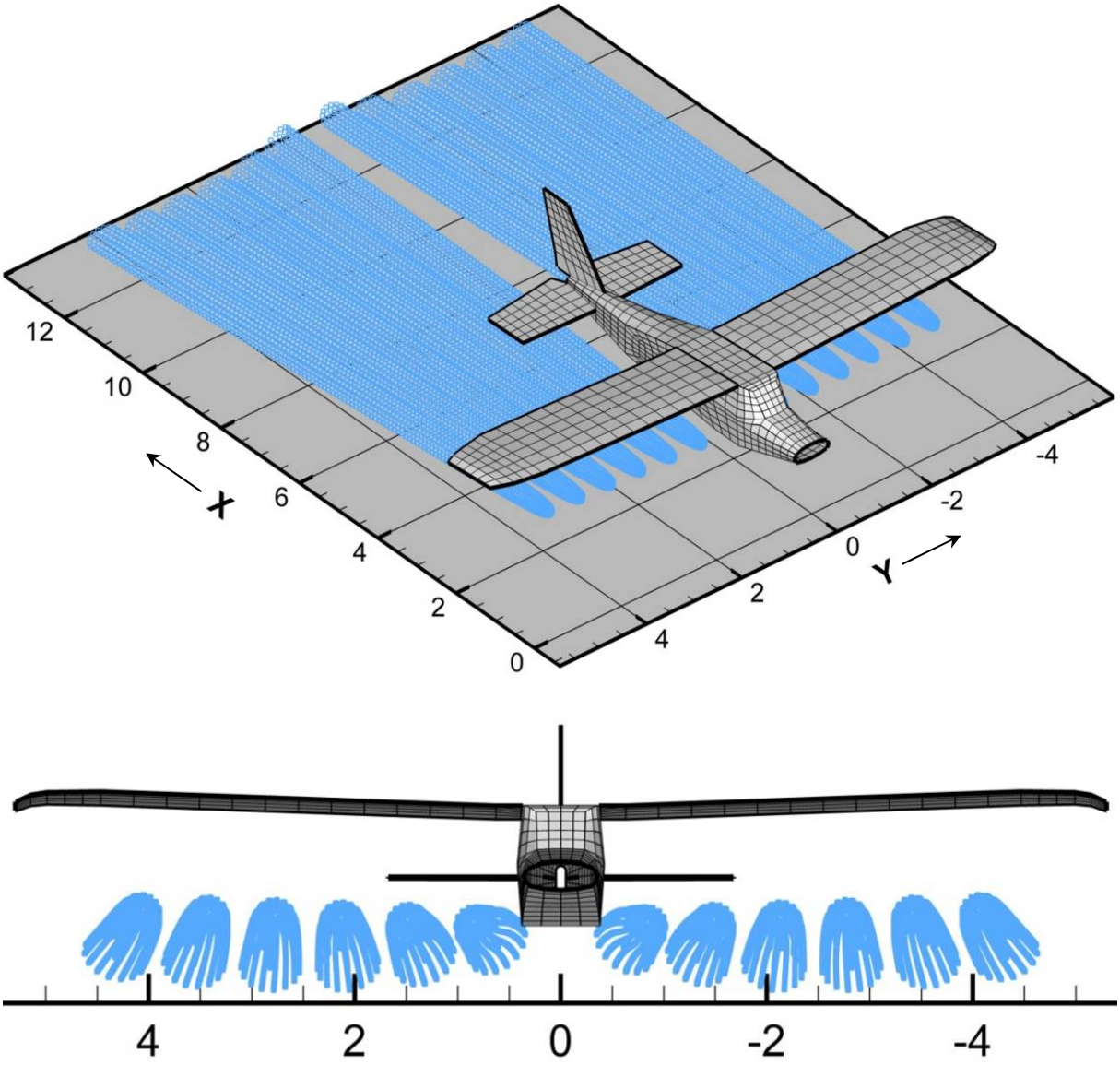

Figure 15: Simulation of aerial application using a typical high-wing airplane.

5 CONSLUSIONS

In this research an original numerical procedure capable of simulating the motion of droplets in the air has been successfully developed and tested. The method has been based on an innovative fusion of two different models: one to reproduce the mechanics of droplets and another one to simulate the airflow. The mechanical model of droplets has been based on an empiric method that allows an easy and precise calculation of the exerted drag force. The unsteady velocity field cause by the motion of a solid body is supplied by an aerodynamic model, which is based on the hypothesis of high Reynolds number and low Mach number.

In association with the numerical methods developed in references Hazebrouck et al. (2010a, b), the new mechanical model of droplets allows the manipulation of the most significant variables that control the efficiency of aerial application systems. Through several examples, the numerical tool has demonstrated to be capable of predicting the distribution of droplets over the ground and the interference caused by each of the components of the aerial system.

REFERENCES

Carnahan, B., Luther, H.A. and Wilkes, J.O., *Applied Numerical Methods.* New York: John Wiley & Sons, Inc. 1969.

Clayton, J.S. (n.d.). New developments in rotary atomisers for improved drift control. Herefordshire, England: Micron Sprayers Ltd.

Hazebrouck, Preidikman, Massa.. *Desarrollo de un software de aerodinámica basado en el método inestacionario de la red de vórtices.* Córdoba: CAIA II. (2010a)

Hazebrouck, Preidikman, Massa. *Desarrollo de una herramienta computacional para el estudio de la eficiencia de la aerofumigación empleando aeronaves monoplano.* Mar del plata: CATE 2009, Asociación Argentina de Tecnología Espacial. 2009.

Hazebrouck, Preidikman, Massa. *Numerical simulations of aerial application systems: developing of models and their applications.* Córdoba: CAIA 2010. 2010b.

Hewitt, A. J. *The importance of nozzle selection and droplet size control in spray application.* Univ. Maine, ME USA. Ed. D Buckley.: North American conference on spray drift management. 1998.

Katz, Plotking. *Low Speed Aerodynamics, From Wing Theory to Panel Methods.* San Diego: McGraw-Hill, 1991.

Milne-Thompson, L.M.. *Theoretical aerodynamics.* New York: Dover Publications, Inc. 1973

Preidikman, S., *Numerical Simulations of Interactions Among Aerodynamics, Structural, Dynamics, and Control Systems.* Doctoral Dissertation. 1998

Zahm, A.F.. *Report No. 253: Flow and drag formulas for simple quadrics.* NACA. 1926